Title:

Hiding in Plain Sight: Thymic CD8+FOXP3+Tregs sequester CD25 and are enriched in human tissues

Authors: Lorna B. Jarvis[1], Sarah K. Howlett[1], Valerie Coppard[1], Daniel B. Rainbow[1], Sarah Alkwai[1], Lou Ellis[1], Zoya Georgieva[1], Ondrej Suchanek[2], Hani Mousa[1], Krishnaa Mahbubani[3], Kourosh Saeb-Parsy[3], Linda S. Wicker[4] and Joanne L. Jones[1*]

Affiliations:

1. Dept Clinical Neurosciences, University of Cambridge, Biomedical Campus, Cambridge, UK
2. Molecular Immunity Unit, Department of Medicine, University of Cambridge, Cambridge, UK
3. Department of Surgery, University of Cambridge, and Cambridge Biorepository for Translational Medicine, NIHR Cambridge Biomedical Research Centre, Cambridge, UK
4. JDRF/Wellcome Diabetes and Inflammation Laboratory, Centre for Human Genetics, Nuffield Department of Medicine, NIHR Oxford Biomedical Research Centre, University of Oxford, Oxford, UK

***Corresponding author**: Email jls53@medschl.cam.ac.uk

One Sentence Summary: FOXP3+CD8+Tregs, expressing tissue residency markers and CD25 intracellularly, are enriched in human non-lymphoid tissues.

Abstract:

For decades regulatory T cell (Treg) research has focussed on CD4+FOXP3+ Tregs, whilst characterisation of CD8+FOXP3+ Tregs has been limited by their paucity in blood. Here, by studying 98 tissues from 27 deceased transplant organ donors we demonstrate that despite representing less than 5% of circulating Tregs, fully functional, thymically derived CD8+FOXP3+ Tregs are highly enriched in human tissues particularly in non-lymphoid tissues and bone marrow, where they reside as $CD25^{lo}$/-CD8+CD69+CD103+TLR9+HELIOS+FOXP3+ Tregs. Despite lacking surface CD25 expression, CD8+ Tregs in tissue are demethylated at the FOXP3 TSDR and express CD25 intracellularly. Surface CD25 expression is quickly regained *in vitro*, allowing cell sorting for therapeutic expansion and confirmation of their suppressive function. We suggest that these elusive cells likely play an essential but previously unappreciated role in maintaining peripheral tolerance within human tissues.

Main Text:

Naturally occurring CD4+ Tregs are a specialised subset of CD4+ T cells that play a vital role in regulating the immune system. They are selected in the thymus to self-antigen expressed on MHC-Class II molecules and are capable of suppressing harmful immune responses to self in the periphery, where they play a key role in preventing autoimmunity and maintaining peripheral tolerance (reviewed (*1*)). Naturally-occurring thymic derived Tregs (nTregs) can be distinguished from peripherally induced Tregs (pTregs) by the methylation status of the TSDR (Treg-specific demethylated region) located in intron 1 of the *FOXP3* gene, which is demethylated in nTregs promoting stable FOXP3 expression(*2*).

Multiple CD8+ T cells with suppressive properties have been described both in mice and humans, including CD8+ cells that are $CD28^{lo}$, CD28lo/CD57+(*3*), CD122+(*4*), $CD45RC^{lo}$(*5*), KIR+ (in human)(*6*), Ly49+ (in mice)(*7*) and CD56+/NKT-like (in mice)(*8*). Whilst the CD28lo and $CD45RC^{lo}$ populations have been shown to contain a small subpopulation of FOXP3 expressing cells, the majority of these reported suppressive CD8+ T cells do not express FOXP3 and are thought to suppress via different mechanisms including cytotoxicity (reviewed in (*9*)). There have also been descriptions of CD8+FOXP3+ Tregs, primarily in the context of human tumour microenvironments where increased numbers correlate with worse outcomes (*10*, *11*). They are also known to be highly responsive to IL-2 (demonstrated in both humans and mice *in vivo*) (*12*, *13*) and human CD8+FOXP3+ Tregs can be expanded *in vitro* using DC(*14*) or polyclonal stimulation(*5*). Yet due to their very low frequency in peripheral blood, few in-depth studies have been performed on *ex vivo* CD8+FOXP3+ Tregs from healthy individuals and their origin and role in human immunity remains elusive (reviewed in(*15*)).

In this study we undertook a detailed analysis of the CD8+FOXP3+ T cell compartment in humans. Our findings confirm the long-held assumption that these cells represent the CD8-expressing/MHC class I restricted counterparts of naturally occurring and thymically derived CD4+ Tregs, and that they are distinct from unconventional cytotoxic FOXP3- CD8+ cells that have suppressive capacity (such as CD28-/CD122+ Tregs or those expressing KIRs). Using a combination of high-parameter flow cytometry, transcriptomic analysis, miniaturised suppression assays, TSDR methylation analysis, and by studying tissues from deceased transplant organ donors (including secondary lymphoid, gut and thymic tissue) we demonstrate that human CD8+FOXP3+ cells are thymically derived, highly suppressive, regulatory cells that are enriched within the Treg compartment of human tissues compared to peripheral blood, in particular in non-lymphoid organs such as gut and liver.

Within tissues, in addition to expressing Treg markers such as CTLA-4 and HELIOS, CD8+FOXP3+ cells express markers associated with tissue residency, including CXCR6, CD69 and CD103, indicating that they are the regulatory equivalent of tissue-resident memory T cells (TRMs). They also express CD25 intracellularly but have low or negative surface expression. This may partly explain why they have been overlooked in previous work focussing on CD25hiCD127lo cells. Notably, tissue resident CD8+FOXP3+ Tregs

express high levels of TLR9, suggesting that they may be able to detect and respond to viral or self DNA during infection or tissue injury. Surface CD25 expression was rapidly regained *in vitro,* enabling CD8+Tregs to be sorted from tissues, expanded using therapeutic expansion protocols, and for their suppressive function to be confirmed. Taken together, we propose that CD8+FOXP3+ regulatory cells play a previously unappreciated role in maintaining tissue health in humans, and that they hold promise for tissue specific Treg cellular therapy.

Results

CD8+FOXP3+ Tregs are naturally occurring FOXP3 TSDR-demethylated counterparts of CD4+FOXP3+ Tregs

To better understand the nature of FOXP3 expressing CD8+ T cells in relation to previously reported CD8+ suppressive populations, we undertook deep phenotyping of CD8+FOXP3+ T cells in human peripheral blood, analysing both classical markers of naturally occuring CD4+FOXP3+ Tregs and markers associated with other reported suppressive CD8+ populations.

In agreement with previous studies, human peripheral blood FOXP3+CD8+ T cells were TCRαβ+ T cells. They expressed a similar profile to their FOXP3+CD4+ counterparts (CD25hi, CD127lo, HELIOS+, CTLA-4+) and lacked markers of unconventional cytotoxic-like CD8 Tregs (KIRs, CD56, CD122) and were CD28+ (Fig.1a). Whilst our data confirmed reports that the majority of CD8+FOXP3+ T cells in human blood are CD45RC^{lo}(*5*) (as are FOXP3+CD4+ Tregs), CD45RC status was not specific for CD8+FOXP3+ cells, but rather was a general feature of all memory cells (Fig. 1a and Fig.S1).

As with CD4+ Tregs, CD25hi and CD127lo expression was the best surface phenotype for identifying CD8+FOXP3+ cells. Around 72% of all circulating CD8+FOXP3+ cells could be identified using this gating strategy vs. 90% for CD4+FOXP3+ cells (cells outside this gate were predominantly CD25lo/negative - Fig. 1a and Fig. S1) and 77% vs. 89% of CD8+ and CD4+ cells within the CD25hiCD127lo gate were FOXP3+. Within blood, approximately 2% of CD25hiCD127lo CD3+ cells were CD8+. This aligns with a previous study in psoriasis(*16*). Similar to CD4+CD25hiCD127lo cells, most circulating CD8+CD25hiCD127lo cells were either central memory (CD45RA-CD27+) or naive (CD45RA+CD27+). Although, in keeping with their CD8 lineage, a greater proportion had a terminally differentiated effector RA (TEMRA) phenotype (Fig.1a, b). Overall, CD8+CD25hiCD127lo cells expressed similar levels of canonical Treg markers to their CD4+ counterparts (Fig.1c), with the exception of TIGIT, which was slightly lower and CD31 and CD73 which were slightly higher ($p < 0.05$ Fig.1c). Similar expression patterns were observed when gating on FOXP3+HELIOS+ cells (fig S2), which also demonstrated lower CD25 CD8 Treg expression.

Next, based on surface CD25hi/CD127lo expression, CD4+ and CD8+T cells were sorted from human blood for targeted transcriptomic analysis by Nanostring. These data demonstrated a high degree of similarity with differential gene expression largely confined to genes associated with CD4 vs. CD8 co-receptor expression (Fig.S3). Having established that CD8+CD25hiCD127loFOXP3+ cells likely represent naturally occurring CD8+ counterparts to CD4+ Tregs, we went on to demonstrate their suppressive function *ex vivo* using a miniaturised Treg suppression assay, required because of their low frequency in blood (Fig.1d). Surface-sorted circulating CD8+ Tregs were found to be fully suppressive, capable of suppressing CD4 and CD8 effector proliferation to the same degree as CD4 Tregs (Fig.1d and fig.S4) and pro-inflammatory cytokine production (Fig. 1e) more effectively. Lastly, we were able to demonstrate that *ex vivo* blood-derived human CD127loCD25hiCD8+Tregs contain a high percentage of cells that are TSDR demethylated (like their CD4 counterparts), indicating that they are a stable, thymically-derived Treg population (Fig. 1f).

CD8+FOXP3+ Tregs are thymically- derived, lineage committed CD8+Tregs

To confirm the thymic origin of CD8+FOXP3+ Tregs, we analysed human thymic tissue obtained from 3 adult deceased transplant organ donors. In addition to CD4+ Tregs, and developing CD4+CD8+ double positive (DP) Tregs, CD8 single positive Tregs were detected, accounting for 6-8% of all TCRαβ+FOXP3+ cells in the thymus (Fig. 2a/b). Deep phenotyping revealed that the CD8+FOXP3+ Tregs were HELIOS+CD5hiCD69+TCRab+ mature cells and that they expressed high levels of the transcription factor RUNX3 and low ThPOK, consistent with thymocytes that have undergone thymic selection to MHC class I/peptide complexes (reviewed (*17*)) and are therefore CD8 lineage committed (Fig.2c).

Of note, thymic CD8+FOXP3+ Tregs expressed lower levels of CD25 than their CD4+ counterparts. They also expressed higher levels of the αE integrin CD103, compared to both CD4+FOXP3+ Tregs and CD8+ Teffectors (Fig.2c and fig. S5). Within the CD8+FOXP3+ population no correlation was seen between CD25 and CD103 expression (fig. S6) and CD103+Tregs within the thymus were found to be either CD8 single positive FOXP3+ Tregs, or CD4+CD8+ double positive (DP) Tregs that expressed RUNX3/ low ThPOK suggesting that DP CD103+ Tregs may be CD8+ lineage committed, and precursors of the CD8+ SP Treg (fig. S6).

We flow sorted CD4+, DP and CD8+FOXP3 positive and negative TCRαβ+ thymocytes and analysed them for TSDR demethylation - all 3 FOXP3+ populations were highly demethylated, as expected for thymic Tregs (Fig. 2d). A small percentage of both CD4+ and CD8+ single positive Tregs were observed to express CD45RA (Fig. 2c), likely representing thymocytes closest to thymic egress(*18*).

Next we analysed cord blood (n=3) and in keeping with their thymic origin, a small population of naive (CD27+CD45RA+) CD8+FOXP3+Tregs (and also a very small DP FOXP3+ population) was observed (Fig.2e). These cells expressed HELIOS, but in comparison to cord blood CD4+Tregs, had low CD25

expression and higher CD103 expression (Fig. 2f). CD103 was highly expressed on both CD8+ and DP FOXP3+Tregs compared to CD4+FOXP3+ Tregs and CD4 and CD8 Teffectors (Fig. 2g and fig. S7.). All three cord blood-derived FOXP3+ Treg subsets were highly demethylated at the TSDR (Fig. 2h).

Together with the T-cell activation marker CD69, expression of the αE integrin CD103 defines a recently identified subtype of T cells called “tissue-resident memory (TRM) cells", found particularly in mucosal and barrier sites(*19*, *20*). We therefore questioned whether CD8+FOXP3+ Tregs are destined to home to tissue, and hypothesised that this may explain their paucity in blood. Of note, several other markers relating to tissue homing/migration and residency were observed amongst the most differentially expressed genes between CD8 Tregs and CD4 Tregs and between CD8 Tregs and CD8 Teffectors measured by Nanostring (despite them being sorted from blood, figs. S3 and S8). These included ITGAE (CD103), CD44, CD97 and other “effector” Treg (eTreg) markers associated with antigen experienced Tregs with tissue migratory potential as demonstrated in CD4+ Tregs in mice(*21*, *22*) as well as a number of genes associated with tissue residency and tissue repair programmes in CD4+ Tregs (DUSP4, BATF(*23*–*26*)). We therefore next sought to determine if CD8+FOXP3+ Tregs are enriched in tissues.

CD8+FOXP3 TSDR-demethylated Tregs are enriched in human tissues and co-express tissue residency markers

We undertook an analysis of regulatory T cells across multiple tissues from 27 deceased human transplant organ donors including: thymus, peripheral blood, thoracic and mesenteric lymph node, lung, spleen, fat, kidney, bone marrow (BM), liver, and gut (ileum and intraepithelial (IEL) layer and lamina propria (LP) of the jejunum) (Fig. 3a). A total of 98 tissue samples were studied. Using multiparameter flow cytometry we found that, as a proportion of the CD127loFOXP3+ Treg pool, CD8+ Tregs are indeed significantly enriched in tissues compared to peripheral blood (Fig. 3 b,c and figs. S9-10). In particular liver, gut, kidney, and BM were highly enriched for CD8+ Tregs where on average they accounted for 50%, 76%, 24.6% and 35.3% of all CD127loFOXP3+ cells compared to 4.4% in blood. In contrast, CD8+Tregs were not significantly enriched within the Treg pool in thymus, lymph nodes (LN), spleen, fat or lung, although variability across donors was seen. These findings in part reflect the fact that CD8+ T cells are the dominant T-cell population in certain tissues in our dataset (fig. S11), as has been reported previously (*27*, *28*). However, whereas CD4 Tregs (as a percent of all CD4+ T-cells) are highest in blood (as well as thymus and lung), CD8+ Tregs are particularly underrepresented in blood - despite the reversal of the CD4:CD8 ratio in the blood of our deceased organ transplant donors (Fig. 3 b,c and fig S11).

Next we used FlowAtlas(*29*) an interactive data explorer for dimensionality-reduced high-parameter flow cytometric analysis developed in-house, and used to assess Treg heterogeneity on a subset of our data stained for the Treg markers FOXP3, CD25, HELIOS, CD127, TIGIT, CTLA-4, and tissue resident markers CD69 and CD103 (figs. S12 and S13); this did not include cells extracted from gut tissue. Within the CD4+

Treg compartment two main subpopulations could be seen, representing naive (CD45RA+CD27+) and central memory Tregs (CD45RA-CD27+) (fig. S12). Broader heterogeneity was seen in the CD8+FOXP3+CD127lo compartment which could be separated into five distinct cell populations including (i) naive CD45RA+CD27+ cells, (ii) CM CD45RA-CD27+ cells, (iii) EM CD45RA-CD27- cells, (iv) TEMRA CD45RA+CD27- cells and (v) a CD45RA- population that expressed high levels of CD69 and increased levels of CD103 (Fig 3d-e and fig. S13). This tissue resident population was absent from blood, rare in bone marrow, but seen in spleen and LN and was the dominant population in non-lymphoid tissue (nLT - consisting here of Liver, Lung and Kidney) and thymus. Blood from the deceased organ donors contained mainly CM cells; bone marrow contained TEMRAs, EM and naive cells; LN contained CM cells and tissue resident Tregs (TRTs) and spleen contained a mixture of all five populations (Fig. 3d). Whereas the CM population present in blood expressed CD25 and was mainly HELIOS positive the other CD8+FOXP3+CD127lo subpopulations showed variable HELIOS and low/absent CD25 expression. To better understand this, we further analysed HELIOS and CD25 expression in CD4 and CD8 FOXP3+CD127lo cells across a range of human tissues (Fig. 3f). This showed that, whilst both CD4+ and CD8+ FOXP3+CD127lo cells in blood were predominantly HELIOS and CD25 positive, within non-lymphoid tissues (liver, gut, kidney, BM and fat) CD25 expression was low/absent on the CD8 population, including on FOXP3+CD127lo cells that co-expressed HELIOS. This was also the case for the CD4+FOXP3+CD127lo cells obtained from human gut and fat. Loss of CD25 was not caused by enzymatic tissue dissociation, since CD25 was retained on CD4 Tregs and PBMC treated with and without liberase and collagenase had comparable CD25 levels (fig. S14)

To understand the nature and origin of these populations, we next sorted FOXP3+CD127lo CD4+ and CD8+ cells from blood, spleen and LN tissue from 3 different donors (where we had sufficient cells) by HELIOS and CD25 for TSDR methylation analysis. This demonstrated that regardless of CD25 expression, across tissue compartments, a high proportion of HELIOS+FOXP3+CD8+ cells are TSDR-demethylated, and are therefore, stable, thymically derived Tregs (Fig. 3g). This is in keeping with data previously published for CD4+ Tregs(*30*). The HELIOS-ve CD25-ve DN fraction of CD8 Tregs sorted from the spleen and blood contained a low proportion (20-40%) of TSDR-demethylated cells (Fig. 3g) compared to spleen- and blood-derived CD4 DN Tregs (fig. S15) where approximately 50% of the cells were demethylated at the TSDR. These populations may therefore contain a mixture of thymically derived Tregs, peripherally induced Tregs and contaminating effectors T cells. Given there is no consensus on how to distinguish these populations, we elected to re-calculate the fraction of CD8 Tregs, as a proportion of total Tregs, across our donor tissues based on HELIOS and FOXP3 co-expression (fig. S16). Data showing the proportion of FOXP3+ CD4+ and CD8+ Tregs expressing HELIOS is also shown in fig. S17. Using this conservative definition of a Treg - CD8+FOXP3+HELIOS+ Tregs were still found to be highly enriched as a proportion of total Tregs in tissue, particularly non-lymphoid tissues (Fig. 4a-b), where they expressed high levels of the tissue residency markers CD69, CXCR6 and CD103 compared to their CD4+ counterparts (Fig 4c-d and fig. S18). No difference was seen in CD8+ Treg frequency between

male and females. A trend towards increased CD8+Tregs with age was observed in bone marrow and spleen, although this did not reach statistical significance (fig. S19).

Tissue resident CD8+ Tregs internalise CD25, and co-express TLR9

We were intrigued by the absence of CD25 on the surface of FOXP3+HELIOS+CD8+ Tregs in tissue. In the T effector pool, long-lived memory CD8+ T cells downregulate key effector molecules such as perforins and granzymes, in order to remain quiescent until their reactivation is required (for example in response to secondary viral exposure(*31*, *32*)). We therefore hypothesised that this might also be the case for tissue resident memory FOXP3+CD8+ Tregs, and that internalisation of CD25 may represent a mechanism by which FOXP3+CD8+ Tregs are kept quiescent in non-inflamed tissue.

To test this, we surface stained cells extracted from a range of healthy human tissues with saturating concentrations of two anti-CD25 antibodies conjugated to BB515 (clones MA2.1/2A3), in order to block all surface binding sites . After washing thoroughly, we permeabilized and stained the same cells with the same anti-CD25 clones but on a different fluorochrome (APC), which could now only bind intracellularly. In this way we were able to show that most of the surface CD25 negative CD8+FOXP3+HELIOS+ Tregs in tissue express CD25 intracellularly. Of note, CD25 surface negative CD4+FOXP3+HELIOS+ Tregs in tissue were also found to express CD25 intracellularly. CD25 intracellular expression was not observed in the effector population (Fig. 4e-f).

The lack of CD25 on the surface of CD8+FOXP3+HELIOS+ CD8+Tregs in tissue, made it difficult to isolate CD8+ tissue resident Tregs for functional or transcriptomic analysis. To try to address this we conducted flow cytometric screening of CD8 Tregs in blood and spleen for expression of a number of candidate surface molecules that were noted to be differentially expressed between CD8+ Tregs and CD8+ Teffector cells in our Nanostring data (fig. S8). Since we noted interferon response genes IRF4 and TRAF1 were upregulated in CD8+ Tregs compared to CD8+ effectors, and the proteins encoded by these two genes are downstream of TLR signalling (and TLR agonists have been demonstrated to promote Treg expansion *in vitro*)(*33*) we also screened for TLR expression.

Among the markers tested, none were specific for FOXP3+HELIOS+CD8+ Tregs compared to CD8 Teffs with the exception of TLR9 - which was expressed at similar levels to that seen on CD79b+B-cells (where it is constitutively expressed, fig. S20 and S21). FOXP3+HELIOS+CD8+Tregs that lacked surface CD25 expression were positive for TLR9 whereas CD8+FOXP3- T effector cells did not express TLR9 (Fig. 4d and g). TLR9 was also found to be expressed on the small CD4+FOXP3+HELIOS+ Treg population that lacked surface CD25 expression and the reciprocal relationship between TLR9 and surface CD25 expression was striking (fig. S21). These data suggest that TLR9 is a marker of surface CD25 negative FOXP3+HELIOS+ Tregs. Since CD25- Tregs have been associated with recent activation we checked to see if CD25- Tregs

expressed Ki67, which they did not (fig. S22). As TLR9 is an intracellular TLR it was also not useful for isolating live CD8+ Tregs for functional analysis.

Tissue resident CD8+ Tregs are TSDR demethylated, functionally suppressive, and have therapeutic potential

As long-lived memory CD8+ T cells retain the capacity to re-express their key effector molecules, we considered that CD8+ tissue Tregs might regain surface CD25 expression once removed from their tissue environment. To test this, splenocytes were removed from their tissue microenvironment and rested for 24h at 37°C. As hypothesised, surface CD25 expression was regained. Interestingly, where surface CD25 expression was acquired, intracellular CD25 levels reduced, and TLR9 expression was lost, confirming their reciprocal relationship (Fig.5a-c). Recovery of surface CD25 expression after a brief resting period opened up the possibility of sorting CD8+Tregs from human tissues for TSDR demethylation analysis and to test their suppressive function *in vitro* (Fig. 5d-e). To do this, CD4 and CD8 CD127loCD25hi Tregs were sorted from human spleen, LN and gut MNCs after resting overnight at 37oC (Fig. 5e). In keeping with our previous data, CD4 and CD8 Tregs recovered from human spleen were fully TSDR demethylated, as were cells recovered from LN (Fig. 5f). In the gut, <50% of the recovered CD127loCD25hi CD8 Tregs were fully TSDR demethylated (Fig. 5f), meaning only half were of thymic origin. This was also the case for the gut isolated CD127loCD25hi CD4 Tregs. Of note, human gut contains a high proportion of HELIOS- FOXP3+ cells, which like their HELIOS+ counterparts, are largely surface CD25 negative, intracellular-CD25+ and TLR9+ *ex vivo* (Fig. 5g; and fig. S23). We therefore propose that these cells are peripherally induced, non-TSDR-demethylated Tregs, and that the gut Treg population is comprised of a mixture of thymically derived and induced regulatory cells. This is in keeping with the literature that has identified the gut as an important site of induced Treg generation(*34*). Given the very low cell numbers available from the gut tissue, it was not possible to split the recovered surface CD25+ Tregs by HELIOS expression for TSDR methylation analysis.

Next, surface CD25 recovered CD127lo CD3+ splenic Tregs (containing a mixture of CD4 and CD8 Tregs) or CD4+ and CD8+ Tregs sorted separately, were expanded using a standard therapeutic expansion protocol involving TCR polyclonal stimulation in the presence of IL-2, and their expansion rate, their phenotype and suppressive capacity after three rounds of expansion were compared and contrasted. Despite representing only a small fraction of the starting population, CD8+ Tregs in bulk cultures expanded more rapidly than their CD4+ counterparts (Fig. 5h). They also maintained their suppressive phenotype, including surface expression of CD25 (HELIOS+FOXP3+CD127lowCD25hiTLR9-) (fig. S24). CD39 expression was similar between expanded splenic CD4 and CD8 Tregs, but CD73 expression (and therefore CD39/CD73 co-expression) was higher on expanded CD8 Tregs compared to CD4 Tregs (fig. S24). We have previously reported that co-expression of the ectonucleosidases CD39/CD73 (which together convert extracellular ATP to immunosuppressive adenosine) is an important mechanism by which therapeutically expanded Tregs

suppress(*35*)). After 3 rounds of expansion, CD4 and CD8 Tregs were sorted from the bulk expansion and their functional suppressive capacity tested in a standard in vitro Treg suppression assay. Splenic CD25 recovered CD127lo CD8+ Tregs were found to be highly suppressive, more so than splenic CD4+ Tregs from the same donor (Fig 5i).

Discussion

In conclusion, we have shown for the first time that, whilst rare in peripheral blood, FOXP3+CD8 Tregs are enriched in human tissues, as a proportion of all Tregs, particularly non-lymphoid tissue where they likely play a key role in maintaining human tissue health and homeostasis.

The existence of CD8+FOXP3+ Tregs has been known for some time. In particular they have been described in the setting of tumours where their presence correlates with poor outcome. They have also been shown to expand in response to low-dose IL-2 in both murine and human studies(*12*, *13*). However their relative abundance in non-lymphoid organs and their likely role in tissue immunity has not been described before and is an important new finding. Lack of awareness of these cells is likely due to an historical focus on CD4+ Tregs, the assumption that all Tregs express high levels of CD25, the fact that tissue resident cells tend to accumulate with age (reducing the likelihood of detecting these cells in young mice housed in sterile environments) and due to the challenges in accessing human healthy tissue

Our initial experiments demonstrated that blood-derived CD4 and CD8 Tregs express comparable levels of canonical Treg-associated molecules both transcriptomically and at the protein level. We also demonstrated that, like CD4+ Tregs, a high proportion of CD8 Tregs (sorted on the basis of either CD25 or FOXP3 and low CD127 expression) are demethylated at the TSDR, suggesting that peripheral blood Tregs are mostly thymically derived. This was confirmed by studying human thymic tissue and by demonstrating the presence of CD8+Tregs in cord blood. Our data also suggested the potential for CD8 Tregs to home to tissue. In particular we observed high CD103 expression on thymic and cord blood derived CD8 Tregs which was not seen on CD4 Tregs or T effector populations. ITGAE (CD103) and several other genes associated with tissue homing and residency were also observed to be differentially expressed in our nanostring data from peripheral blood-derived CD8+ Tregs, including DUSP4 and BATF(*23*, *24*). In addition, CD103 expression on FOXP3+ CD4/CD8 double positive thymocytes also indicated CD8 lineage commitment. These results align with observations reported by Nunes-Cabaço et al(*36*)

To test the hypothesis that CD103+ CD8 Tregs home to tissue, we performed multi-parameter flow cytometry on 98 tissues obtained from 27 deceased organ donors. This extensive and rare dataset confirmed CD8 Treg relative enrichment in tissue - particularly non-lymphoid tissue and especially in the gut, where they were also observed to express CD69 and CXCR6. Whilst a proportion of FOXP3+ CD8 and CD4 Tregs across all tissues

were found to lack HELIOS expression, this population was particularly enriched in the gut. Only half of the gut derived CD4 and CD8 Tregs were found to be TSDR demethylated. Whilst we were unable to split the recovered Treg population by HELIOS expression (due to very low cell number) these data fit with the concept that HELIOS denotes a thymically derived Treg(*37*, *38*) The cellular identity of the FOXP3+ HELIOS- sub-population is unclear and may represent a mixture of activated FOXP3 expressing effectors and induced Tregs. However, recent work from Maja Busko and Ethan Shevach has shown that, in contrast to *in vitro* stimulated cells, FOXP3 is not acquired by activated human conventional T-cells *in vivo*(*39*). Taken together this would suggest that HELIOS-FOXP3+ cells in the gut are induced Tregs. This is consistent with the literature demonstrating that the gut is an important site for Treg induction both in mice and humans (reviewed in (*34*, *40*)).

Compared to peripheral blood, a significant proportion of CD8+FOXP3+ Tregs in tissue lack surface CD25 expression (unrelated to enzymatic dissociation). Why this should be so is unclear, although there are reports of other CD25- Treg populations, including functionally suppressive CD25- T-follicular regulatory cells (CXCR5/PD1hi) in mice and humans(*41*). TSDR demethylated CD25lo CD4+HELIOS+FOXP3+Tregs have also been reported to accumulate in autoimmunity, where their numbers correlate with Treg cell cycle and activation(*30*). Here, we have shown that surface CD25 negative CD8+FOXP3+ Tregs express CD25 intracellularly. This was not tested in previous studies. CD25 was rapidly expressed at the surface on removal from the tissue microenvironment (in vitro), allowing sorting of these cells for functional studies and TSDR methylation analysis.

We also report an inverse relationship between TLR9 expression and surface CD25 expression - a relationship also seen in the CD4 compartment. We have not explained the link between these two molecules (this is a subject of on-going work), but it is interesting to speculate that sensing microbial or self-DNA during the course of infection or tissue injury might be an important part of their function in preventing aberrant immune responses to self antigen (TLR9 has been shown to be able to sense self-DNA/DAMPS in the context of sterile tissue injury(*42*–*44*)). In general little is known about TLR expression by human Tregs. Several studies have reported that TLR9 signalling in APCs has *a* limiting effect on peripherally induced Tregs(*45*, *46*), but very little has been published on the role of TLR9 expression in Tregs themselves. In one study TLR9 was reported to be expressed in a subset of human IL-10 secreting CD4 pTregs (induced in the presence of dexamethasone and VItD3/Calcitriol), and signalling through TLR9 via CpGs inhibited their function by inhibiting IL-10 secretion(*47*) . However, in another study TLR9 expression was identified in *ex vivo* nTregs undergoing therapeutic expansion and TLR9 agonists were shown to promote their function(*33*). Furthermore data from TLR9-/- mice suggest a role for TLR9 in promoting Treg function and migration and retention into tissues. Finally, cobitolimod (which activates TLR9) was recently shown to promote immune regulation in a human colitis IBD trial with improved resolution of colitis(*48*, *49*).

Although we have shown that tissue CD8 Tregs express markers of tissue residency, suggesting that we have identified the regulatory counterpart to TRMs, our data do not speak to the longevity of these cells in tissues. Mouse studies are likely to be of limited value in exploring these questions, given the lack of these cells in mouse tissue. Studying explanted organs after transplant rejection may offer insights directly in humans - but such tissues were not available for this project.

Given that they are highly suppressive, home into tissue and are able to be activated by antigen presented on MHC Class I (expressed by most cells of the body), we suggest that CD8+FOXP3+ Tregs have significant therapeutic potential. A challenge to translation will be their low frequency in blood. However, we have shown that they are enriched within bone marrow (which is clinically accessible) and can be expanded rapidly *in vitro*, even more so than CD4 Tregs, without losing their suppressive phenotype or function. Of note, there is a growing interest in the therapeutic potential of CD8 Tregs. In particular, Guillonneau et al. have shown that human CD8+ Tregs expanded from CD45RClow CD8+ T cells have therapeutic potential despite containing a relatively low frequency of FOXP3+CD8+ T cells(*5*). This group and others have also demonstrated that engineering Tregs with chimeric antigen receptors that specifically recognise MHC Class I can promote immune tolerance of transplanted organs.(*50*, *51*)

In summary - we report for the first time that CD8 FOXP3+ Tregs are enriched in both lymphoid and non-lymphoid human tissues, and are likely the regulatory counterpart of TRMs. This novel finding has significant implications both for the development of novel therapies, but also for the basic understanding of human tissue health and disease.

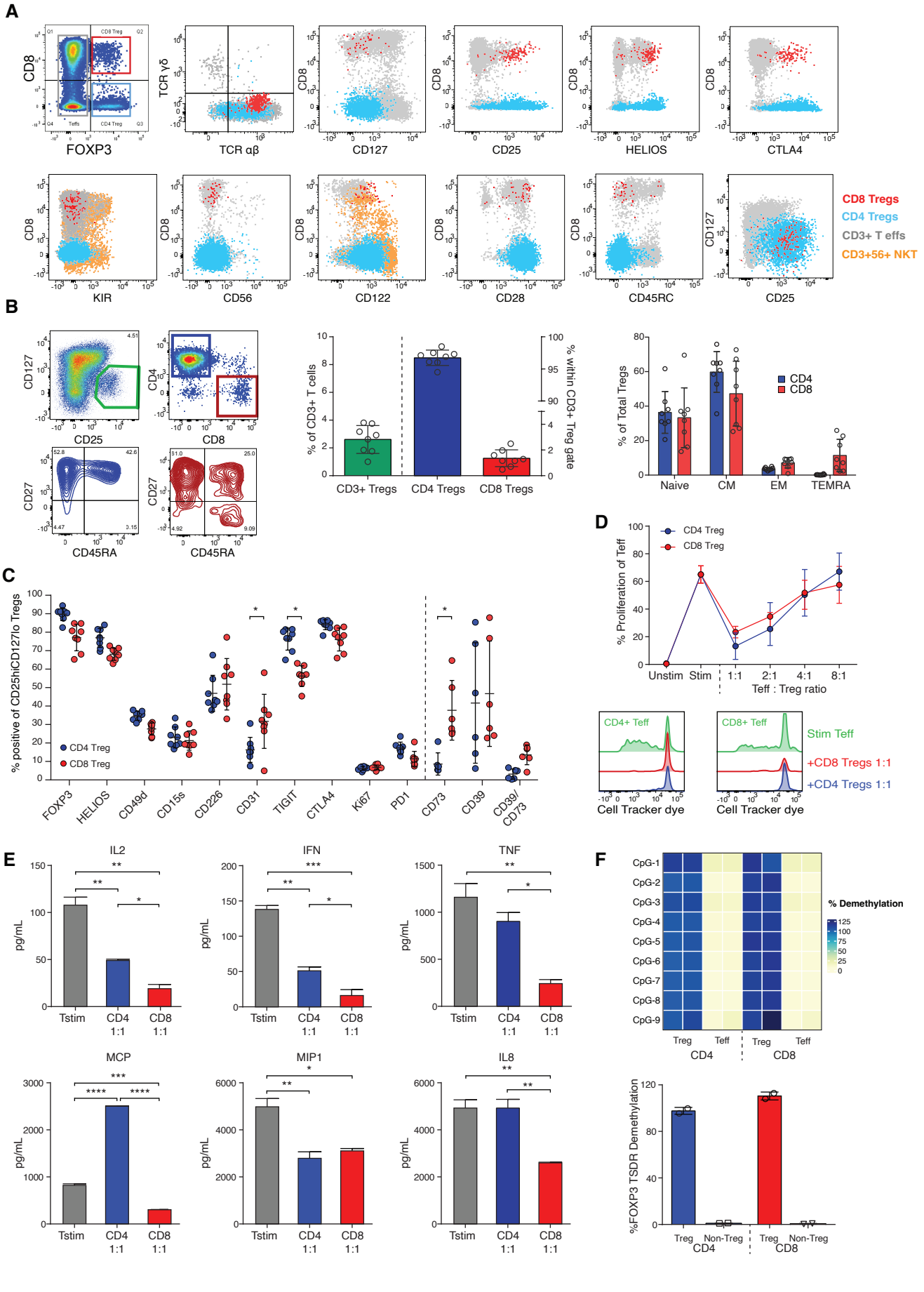
A
CD8
FOXP3
TCR γδ
TCR αβ
CD127
CD25
HELIOS
CTLA4
KIR
CD56
CD122
CD28
CD45RC
CD8 Tregs
CD4 Tregs
CD3+ T effs
CD3+56+ NKT
B
CD127
CD25
CD4
CD8
CD27
CD45RA
% of CD3+ T cells
% within CD3+ Treg gate
CD3+ Tregs
CD4 Tregs
CD8 Tregs
% of Total Tregs
CD4
CD8
Naive
CM
EM
TEMRA
C
% positive of CD25hiCD127lo Tregs
CD4 Treg
CD8 Treg
FOXP3
HELIOS
CD49d
CD15s
CD226
CD31
TIGIT
CTLA4
Ki67
PD1
CD73
CD39
CD39/ CD73
D
% Proliferation of Teff
CD4 Treg
CD8 Treg
Unstim
Stim
1:1
2:1
4:1
8:1
Teff : Treg ratio
CD4+ Teff
CD8+ Teff
Stim Teff
+CD8 Tregs 1:1
+CD4 Tregs 1:1
Cell Tracker dye
Cell Tracker dye
E
IL2
IFN
TNF
MCP
MIP1
IL8
pg/mL
Tstim
CD4 1:1
CD8 1:1
F
CpG-1
CpG-2
CpG-3
CpG-4
CpG-5
CpG-6
CpG-7
CpG-8
CpG-9
% Demethylation
Treg
Teff
CD4
CD8
%FOXP3 TSDR Demethylation
Treg
Non-Treg
CD4
CD8

Figure 1 CD8+FOXP3+ Tregs in human blood are functionally suppressive and TSDR demethylated

A: Representative example of FOXP3+ staining in human PBMC (gated on live CD3+ T cells) and comparison of canonical and unconventional CD8+ regulatory cell markers by flow cytometry. Dotplot overlays show gated CD3+CD4+FOXP3+ Tregs (blue); CD3+CD8+FOXP3+ Tregs (red), FOXP3-CD3+ T cells (grey) and CD56+CD3+ cells (orange). n = 3 donors

B: Proportion of CD3+CD25hiCD127lo CD4+ (blue) and CD8+ cells (red) in human PBMC (top) and distribution of naive and memory subsets in that compartment based on expression of CD27 and CD45RA expression CD4+ (blue) and CD8+ (red) (bottom). Representative gating (left) and summary plots (right) of n = 8 donors. Bar charts show mean +/- SD.

C: Comparison of Treg canonical markers between CD4+ and CD8+ Tregs (gated on CD3+CD25hiCD127lo Tregs) in human PBMC. Percentage positive of total CD4+ (blue) or CD8+ (red) Tregs are presented, n = 8 donors. Data shows mean +/- SD and statistical differences were assessed using multiple T-tests with Holm-sidak correction method.

D: Proliferation of stimulated and tracker dye labelled pan T (CD3+) effector T cells cultured with and without either CD4+CD25hiCD127lo (blue) or CD8+CD25hiCD127lo (red) Tregs flow sorted from human PBMC. Summary of3 donors showing mean % proliferation +/- SD (top) and representative histograms showing suppression of both CD4 and CD8 T effectors (bottom)

E: Cytokine production of stimulated human pan T (CD3+) T effector cells (black) cultured with and without either CD4+ Tregs (blue bars) or CD8+ Tregs (red bars), summary of 2 donors. Data shows mean +/- SD. Comparisons were made using one way ANOVA with Tukey's multiple comparisons test.

F:TSDR demethylation of human *ex vivo* CD3+CD4+CD25hiCD127lo and CD3+CD8+CD25hiCD127lo Tregs sorted from PBMC (n = 4 donors).

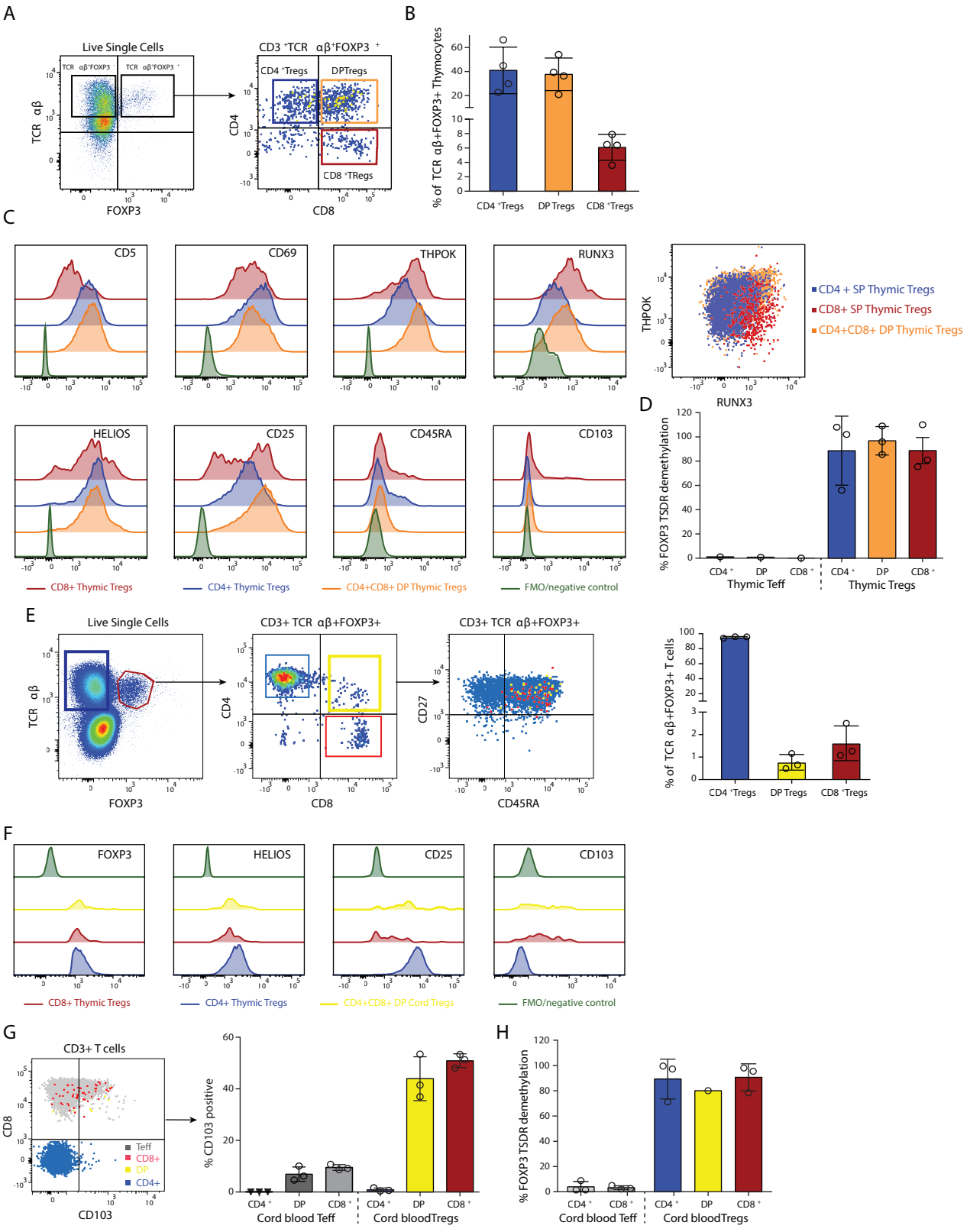
A
Live Single Cells
TCR αβ+FOXP3
TCR αβ+FOXP3+
TCR αβ
FOXP3
CD3+TCR αβ+FOXP3+
CD4+Tregs
DPTregs
CD8+TRegs
CD4
CD8
B
% of TCR αβ+FOXP3+ Thymocytes
CD4+Tregs
DP Tregs
CD8+Tregs
C
CD5
CD69
THPOK
RUNX3
HELIOS
CD25
CD45RA
CD103
CD8+ Thymic Tregs
CD4+ Thymic Tregs
CD4+CD8+ DP Thymic Tregs
FMO/negative control
CD4 + SP Thymic Tregs
CD8+ SP Thymic Tregs
CD4+CD8+ DP Thymic Tregs
D
% FOXP3 TSDR demethylation
CD4+
DP
CD8+
Thymic Teff
Thymic Tregs
E
Live Single Cells
CD3+ TCR αβ+FOXP3+
CD27
CD45RA
% of TCR αβ+FOXP3+ T cells
F
FOXP3
CD4+CD8+ DP Cord Tregs
G
CD3+ T cells
Teff
CD8+
DP
CD4+
% CD103 positive
Cord blood Teff
Cord bloodTregs
H
% FOXP3 TSDR demethylation
Cord blood Teff
Cord bloodTregs

Figure 2 Fully demethylated CD8+FOXP3+ Tregs are thymic derived and exist in early life in humans

A: Representative flow cytometric staining of TCRαβ vs FOXP3 staining on live lymphocytes (left) and identification of CD4, CD8 and DP TCRαβ+FOXP3+ T cells in human thymus (right)

B: Percentage of CD4+ SP (blue), CD4+CD8+ DP (orange) and CD8+SP (red) FOXP3+ cells in human thymus (n = 3 donors). Bars show mean +/-SD.

C: Flow staining of canonical Treg and mature thymocyte markers and transcription factors THPOK and RUNX3 CD4+ (blue), CD8+ (red) and DP+ (orange) FOXP3+ thymocytes compared with unstained or FMO controls (green). Representative example of 3 donors.

D: Histogram showing percentage FOXP3 TSDR demethylation in flow sorted TCRαβ+ FOXP3+ CD4+(blue), CD8+ (red) and DP (orange) thymocytes compared with FOXP3- Teffector counterparts (mean values + SD are shown, summary of 3 donors).

E: TCRαβ vs FOXP3 staining on live lymphocytes (left dotplot), CD4 vs CD8 staining on CD3+FOXP3+ cells (middle dotplot) and CD27 vs CD45RA staining (right plot) of human cord-blood. Representative example of 3 donors. Percentage of CD4+ SP (blue), CD4+CD8+ DP (yellow) and CD8+SP (red) FOXP3+ cells in human cord blood (right hand histogram, n = 3 donora). Bars show mean +/-SD.

F: :Flow cytometric phenotyping of cord blood TCRαβ+FOXP3+ Tregs comparing CD4+ (blue), CD8+ (red) and DP+ (yellow) with unstained or FMO controls (green). Representative example of 3 donors.

G: Dotplot overlays showing expression of CD8 vs CD103 in CD4+FOXP3+TCRαβ+ Tregs (blue), CD8+FOXP3+TCRαβ+ Tregs (red) and CD4+CD8+ (DP) FOXP3+TCRαβ+ Tregs (yellow), representative example of 3 donors. Histogram shows summary data for percentage CD103 positivity within Treg and Teff gates (n = 3 donors).

H: Histograms showing % FOXP3 TSDR demethylation in flow sorted TCRαβ+ FOXP3+CD4+(blue), CD8+ (red) and DP (yellow) cord blood Tregs (summary of 3 donors) and in gated TCRαβ+ FOXP3+CD4+(blue), CD8+ (red) and DP (yellow) cord blood Tregs and their Teffector counterparts (right plot, summary of 3 donors). Values shown are mean +/- SD.

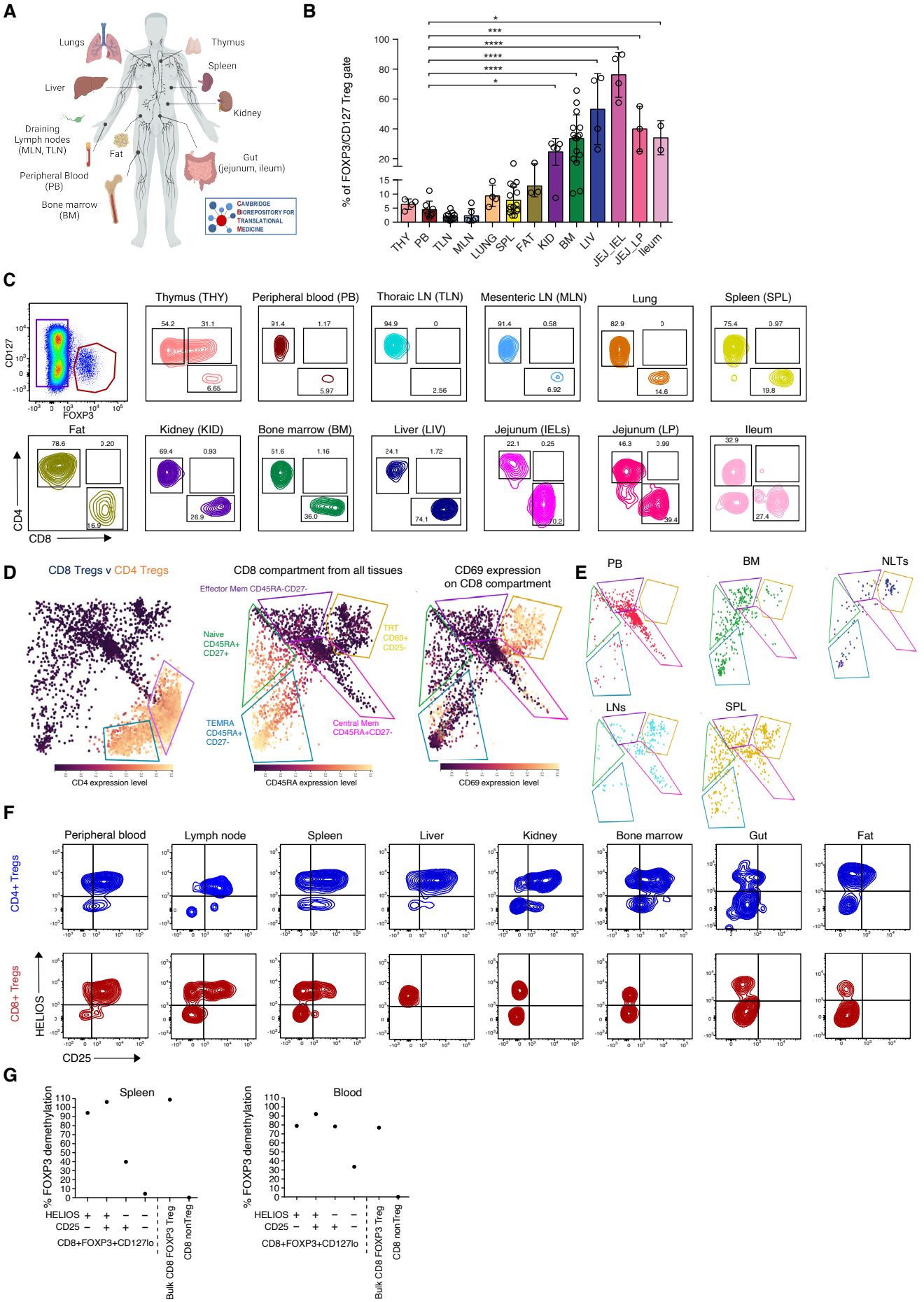
A
Lungs
Thymus
Spleen
Liver
Kidney
Draining Lymph nodes (MLN, TLN)
Fat
Gut (jejunum, ileum)
Peripheral Blood (PB)
Bone marrow (BM)
CAMBRIDGE BIOREPOSITORY FOR TRANSLATIONAL MEDICINE
B
% of FOXP3/CD127 Treg gate
THY
PB
TLN
MLN
LUNG
SPL
FAT
KID
BM
LIV
JEJ_IEL
JEJ_LP
Ileum
C
Thymus (THY)
Peripheral blood (PB)
Thoraic LN (TLN)
Mesenteric LN (MLN)
Lung
Spleen (SPL)
Fat
Kidney (KID)
Bone marrow (BM)
Liver (LIV)
Jejunum (IELs)
Jejunum (LP)
Ileum
CD127
FOXP3
CD4
CD8
D
CD8 Tregs v CD4 Tregs
CD8 compartment from all tissues
CD69 expression on CD8 compartment
Effector Mem CD45RA-CD27-
Naive CD45RA+ CD27+
TRT CD69+ CD25-
TEMRA CD45RA+ CD27-
Central Mem CD45RA+CD27-
CD4 expression level
CD45RA expression level
CD69 expression level
E
PB
BM
NLTs
LNs
SPL
F
Peripheral blood
Lymph node
Spleen
Liver
Kidney
Bone marrow
Gut
Fat
CD4+ Tregs
CD8+ Tregs
HELIOS
CD25
G
Spleen
Blood
% FOXP3 demethylation
HELIOS
CD25
CD8+FOXP3+CD127lo
Bulk CD8 FOXP3 Treg
CD8 nonTreg

Figure 3 CD8+CD127loFOXP3+ Tregs are enriched in Human tissues and are TSDR demethylated

A: Schematic showing tissues harvested by the Cambridge Biorepository for Translational Medicine (Cambridge) from 21 deceased organ transplant donors, produced using Biorender.

B: Summary of % CD8+ Tregs within live, CD3+FOXP3+CD127lo gated T cells across different human tissues (n = 4 Thymus; 8 PBMC; 14 TLN; 12 MLN; .4 LUNG; 16 spleen; 3 Fat; 5 Kidney; 17 BM; 5 LIVER; 4 Jejunum IELs; 4 Jejunum LP and 2 ileum). Bar charts and error bars show mean +/- SD with individual data points shown. Statistical differences were assessed using One Way ANOVA with Tukey's multiple comparisons test.

C: Representative example of CD127 vs FOXP3 staining on live CD3+ T cells (dotplot) and proportion of CD4 vs CD8+ Tregs across multiple organs and tissues (representative contour plots, one per tissue).

D: FlowAtlas analysis of T cell compartment in n = 40 cross-sectional tissues from 20 donors. CD4 expression level is shown in Orange (left plot) and FlowAtlas analysis of CD8+FOXP3+CD127lo gated Tregs from the same donors (middle and right hand plots). Middle plot shows CD45RA expression levels, and identification of 5 subpopulations within the CD8+ Treg pool and the right hand plot shows expression levels of CD69 within the 5 subpoulations of CD8+ Tregs.

E: Representation of CD8+ Treg subsets across human tissues by organ (peripheral blood = red; BM = green; non-lymphoid tissues (lung, kidney, liver) = purple; lymph nodes = blue and spleen = yellow)

F: Representative plots of CD25 v HELIOS expression in CD4+FOXP3+CD127lo (blue) and CD8+FOXP3+CD127lo (red) Tregs across human tissues (representative plots of at least 3 donors per tissue).

G: Percentage TSDR demethylation of CD3+CD8+FOXP3+CD127lo Treg subpopulations based on expression of CD25 and HELIOS in human spleen and peripheral blood.

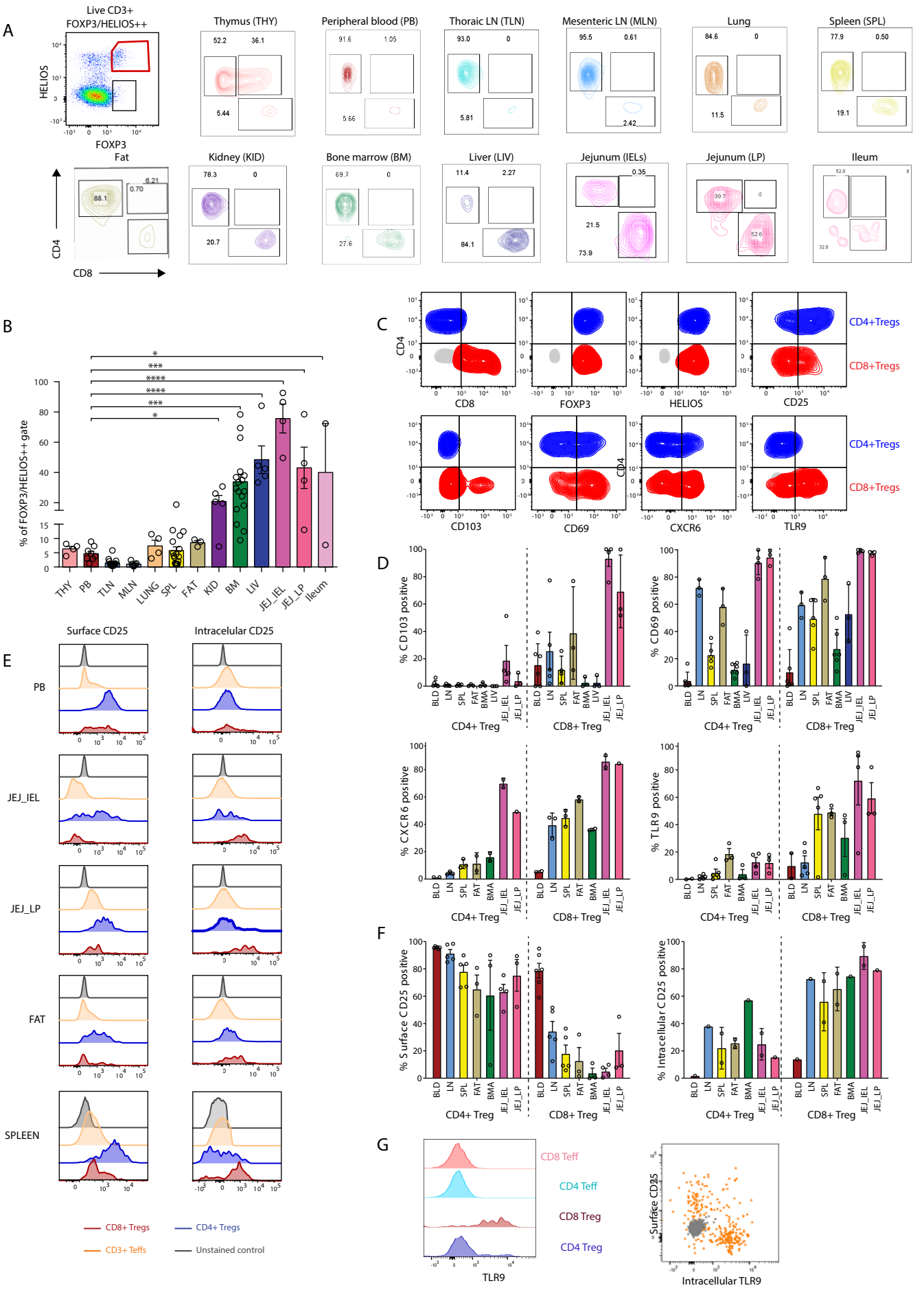
A
Live CD3+
FOXP3/HELIOS++
HELIOS
FOXP3
Thymus (THY)
Peripheral blood (PB)
Thoraic LN (TLN)
Mesenteric LN (MLN)
Lung
Spleen (SPL)
Fat
Kidney (KID)
Bone marrow (BM)
Liver (LIV)
Jejunum (IELs)
Jejunum (LP)
Ileum
CD4
CD8
B
% of FOXP3/HELIOS++ gate
THY
PB
TLN
MLN
LUNG
SPL
FAT
KID
BM
LIV
JEJ_IEL
JEJ_LP
Ileum
C
CD4+Tregs
CD8+Tregs
CD8
FOXP3
HELIOS
CD25
CD103
CD69
CXCR6
TLR9
D
% CD103 positive
% CD69 positive
% CXCR6 positive
% TLR9 positive
CD4+ Treg
CD8+ Treg
BLD
LN
SPL
FAT
BMA
LIV
JEJ_IEL
JEJ_LP
E
Surface CD25
Intracelular CD25
PB
JEJ_IEL
JEJ_LP
FAT
SPLEEN
CD8+ Tregs
CD4+ Tregs
CD3+ Teffs
Unstained control
F
% Surface CD25 positive
% Intracellular CD25 positive
G
CD8 Teff
CD4 Teff
CD8 Treg
CD4 Treg
TLR9
Surface CD25
Intracellular TLR9

Figure 4 Tissue resident CD8+CD127loFOXP3+ Tregs express tissue residency markers and intracellular CD25 and TLR9

A: Representative example of FOXP3vs HELIOS staining of live CD3+ T cells (dotplot) and proportion of CD4 vs CD8+ Tregs across multiple organs and tissues (representative contour plots, one per tissue).

B, Percentage of CD8+ Tregs within CD3+FOXP3+HELIOS+ gated cells across different human tissues (n = 4 Thymus; 8 PBMC; 14 TLN; 12 MLN; .4 LUNG; 16 spleen; 3 Fat; 5 Kidney; 17 BM; 5LIVER; 4 Jejunum IELs; 4 Jejunum LP and 2 ileum). One Way ANOVA with Tukey's multiple comparisons test.

C: Expression of tissue resident markers by CD4+ (blue) and CD8+ (red) CD3+FOXP3+HELIOS+ gated Tregs in human tissues. Contour plots show representative CD4 v canonical Treg and tissue resident markers.

D: Summary plots of %CXCR6, CD69, CD103 and intracellular TLR9 positive cells within CD4 Treg (blue) and CD8+ Treg (red) subsets gated on CD3+FOXP3+HELIOS+ cells, 2-3 donors and 7 tissues. Bars show mean +- SD.

E: Histogram showing surface (left plots) vs Intracellular (right plot) CD25 staining on gated CD4+ (blue) and CD8+ (red) CD3+FOXP3+HELIOS+ Tregs in 5 representative human tissues. Grey histograms show unstained control and orange histograms show Teffector (CD3+Non-FOXP3+) cells.

F: Summary of surface and intracellular expression of CD25 in human CD4+ and CD8+ CD3+FOXP3+HELIOS+ Tregs in human tissues (24 tissues from 5 donors for Surface_CD25 and 10 tissues from 2 donors for intracellular_CD25). Bars show mean values +/- SD.

G: Intracellular TLR9 expression by flow cytometry of gated CD3+CD4+ (blue) and CD8+ (red) FOXP3+HELIOS+ Tregs and FOXP3- Teffectors (left plot) and TLR9 vs surface CD25 expression in CD3+FOXP3+HELIOS+ gated bulk Tregs in representative sample (Spleen) (right plot).

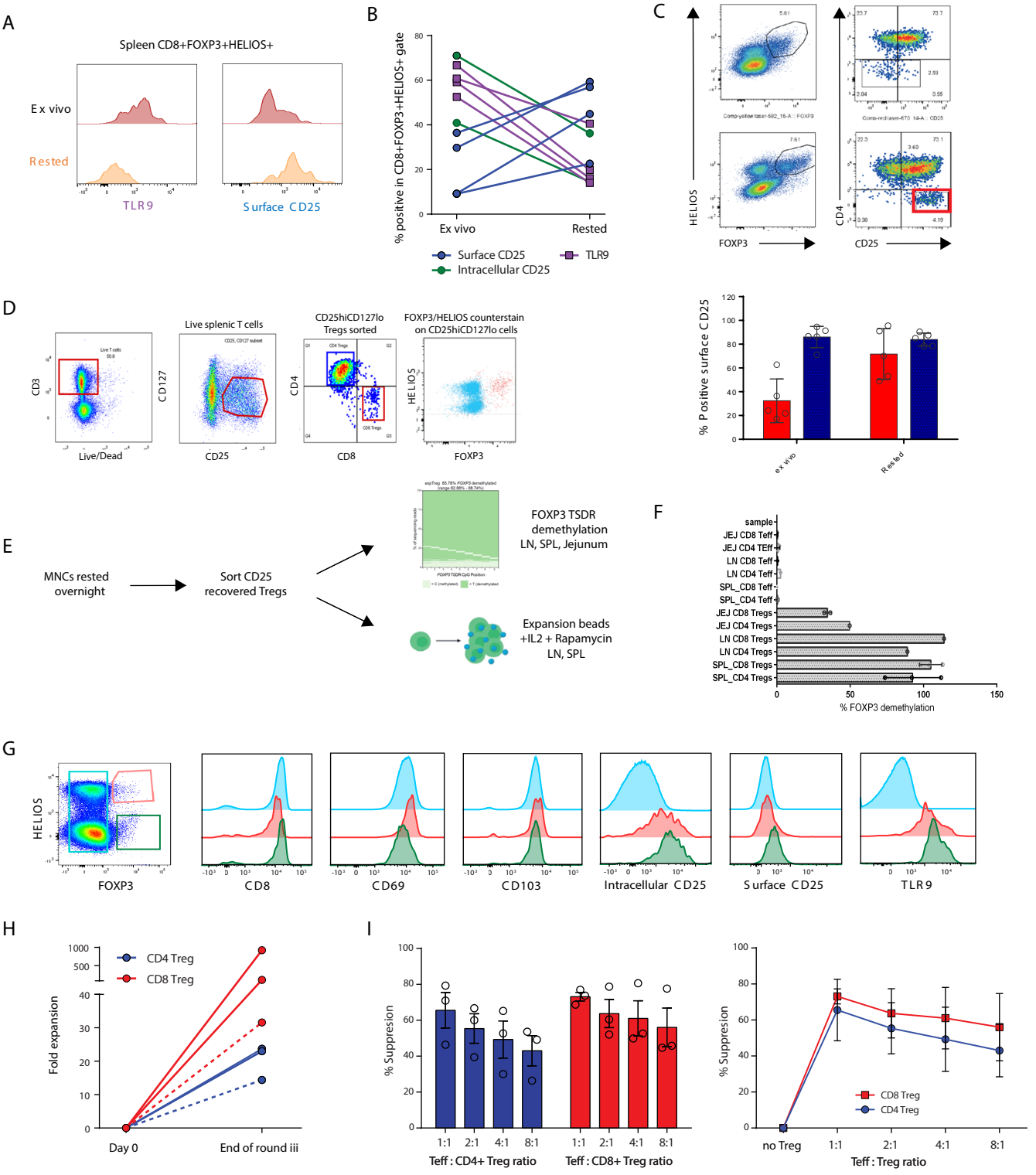
A
Spleen CD8+FOXP3+HELIOS+
Ex vivo
Rested
TLR9
Surface CD25
B
% positive in CD8+FOXP3+HELIOS+ gate
Ex vivo
Rested
Surface CD25
Intracellular CD25
TLR9
C
HELIOS
FOXP3
CD4
CD25
D
Live splenic T cells
CD25hiCD127lo Tregs sorted
FOXP3/HELIOS counterstain on CD25hiCD127lo cells
CD3
CD127
Live/Dead
CD25
CD4
CD8
HELIOS
FOXP3
% Positive surface CD25
ex vivo
Rested
E
MNCs rested overnight
Sort CD25 recovered Tregs
FOXP3 TSDR demethylation LN, SPL, Jejunum
Expansion beads +IL2 + Rapamycin LN, SPL
F
sample
JEJ CD8 Teff
JEJ CD4 TEff
LN CD8 Teff
LN CD4 Teff
SPL_CD8 Teff
SPL_CD4 Teff
JEJ CD8 Tregs
JEJ CD4 Tregs
LN CD8 Tregs
LN CD4 Tregs
SPL_CD8 Tregs
SPL_CD4 Tregs
% FOXP3 demethylation
G
HELIOS
FOXP3
CD8
CD69
CD103
Intracellular CD25
Surface CD25
TLR9
H
CD4 Treg
CD8 Treg
Fold expansion
Day 0
End of round iii
I
% Suppresion
Teff : CD4+ Treg ratio
Teff : CD8+ Treg ratio
CD8 Treg
CD4 Treg
no Treg
Teff : Treg ratio

Figure 5 Tissue resident CD8+ Tregs (TRTs) regain surface CD25 expression and are functionally suppressive and TSDR demethylated.

A: TLR9 (left plot) and surface CD25 (right plot) expression on gated CD3+FOXP3+HELIOS+CD8+ Tregs in human splenic MNCs stained directly *ex vivo* (brown histogram) and after 24h rest at 37oC (orange histogram)

B: Summary data for surface CD25 (blue), intracellular CD25 (green) and TLR9 (pink) expression pre and post-resting for 2-4 donors.

C: Dotplot showing surface CD25 expression on human splenic bulk CD3+FOXP3+HELIOS+ Tregs before (top plots) and after (bottom plots) resting and summary histogram for recovery of surface CD25 on 5 human spleens. Bars show Mean % surface CD25 expression +/SD.

D: MNCs rested overnight at 37oC and live CD3+_CD27lo_recovered Surface CD25+ CD4+ and CD8+ Tregs separated by cell surface flow sorting. A small amount of sample was counterstained for intracellular FOXP3/HELIOS to demonstrate that sorted Tregs were FOXP3/HELIOS++.

E: Schematic demonstrating protocol for isolating CD4 and CD8+ Tregs from human tissues. Sorted Tregs were taken forward for TSDR demethylation analysis and, where cell number allowed, therapeutic Treg expansion in vitro.

F: Post-surface CD25 recovery surface sorted CD3+CD25hiCD127lo CD4+ and CD8+ Tregs and CD3+CD25- CD4+ and CD8+ Teffector cells were assessed for TSDR demethylation. % TSDR demethylation in Jejunum (2 donors); LN (1 donor) and spleen (3 donors). Bars show mean +/- SD.

G: Comparison of gut CD3+ Teffector (FOXP3-), FOXP3+HELIOS+ Tregs (red) and FOXP3+HELIOS- Tregs (green) for CD69, CD103, surface and intracellular CD25 and TLR9. Representative example of 2 donors

H: Expansion rate of CD4+ (blue) and CD8+ (red) Tregs expanded from 3 donors after 3 rounds of expansion either as flow sorted bulk CD3+CD25hiCD127lo human splenocytes (solid lines) or as separated CD4+ and CD8+. CD3+CD25hiCD127lo populations (dotted lines).

I: Suppression of proliferation of CT_efluor450 labelled and anti-CD3/28 stimulated pan T cells in co-culture with either CD4 or CD8+ splenic derived expanded Tregs. Summary of 3 human spleen-derived expTregs with bars representing mean +/-SD.

References and Notes:

References:

1. J. Pohar, Q. Simon, S. Fillatreau, Antigen-Specificity in the Thymic Development and Peripheral Activity of CD4+FOXP3+ T Regulatory Cells. *Front. Immunol.* **9** (2018).
2. J. K. Polansky, K. Kretschmer, J. Freyer, S. Floess, A. Garbe, U. Baron, S. Olek, A. Hamann, H. von Boehmer, J. Huehn, DNA methylation controls Foxp3 gene expression. *Eur. J. Immunol.* **38**, 1654–1663 (2008).
3. M. Strioga, V. Pasukoniene, D. Characiejus, CD8+ CD28− and CD8+ CD57+ T cells and their role in health and disease. *Immunology* **134**, 17–32 (2011).
4. M. Rifa'i, Y. Kawamoto, I. Nakashima, H. Suzuki, Essential Roles of CD8+CD122+ Regulatory T Cells in the Maintenance of T Cell Homeostasis. *J. Exp. Med.* **200**, 1123–1134 (2004).
5. S. Bézie, D. Meistermann, L. Boucault, S. Kilens, J. Zoppi, E. Autrusseau, A. Donnart, V. Nerrière-Daguin, F. Bellier-Waast, E. Charpentier, F. Duteille, L. David, I. Anegon, C. Guillonneau, Ex Vivo Expanded Human Non-Cytotoxic CD8+CD45RClow/− Tregs Efficiently Delay Skin Graft Rejection and GVHD in Humanized Mice. *Front. Immunol.* **8** (2018).
6. J. Li, M. Zaslavsky, Y. Su, J. Guo, M. J. Sikora, V. van Unen, A. Christophersen, S.-H. Chiou, L. Chen, J. Li, X. Ji, J. Wilhelmy, A. M. McSween, B. A. Palanski, V. V. A. Mallajosyula, N. A. Bracey, G. K. R. Dhondalay, K. Bhamidipati, J. Pai, L. B. Kipp, J. E. Dunn, S. L. Hauser, J. R. Oksenberg, A. T. Satpathy, W. H. Robinson, C. L. Dekker, L. M. Steinmetz, C. Khosla, P. J. Utz, L. M. Sollid, Y.-H. Chien, J. R. Heath, N. Q. Fernandez-Becker, K. C. Nadeau, N. Saligrama, M. M. Davis, KIR+CD8+ T cells suppress pathogenic T cells and are active in autoimmune diseases and COVID-19. *Science* **0**, eabi9591.
7. H.-J. Kim, X. Wang, S. Radfar, T. J. Sproule, D. C. Roopenian, H. Cantor, CD8+ T regulatory cells express the Ly49 Class I MHC receptor and are defective in autoimmune prone B6-Yaa mice. *Proc. Natl. Acad. Sci.* **108**, 2010–2015 (2011).
8. C. Wang, X. Liu, Z. Li, Y. Chai, Y. Jiang, Q. Wang, Y. Ji, Z. Zhu, Y. Wan, Z. Yuan, Z. Chang, M. Zhang, CD8+NKT-like cells regulate the immune response by killing antigen-bearing DCs. *Sci. Rep.* **5**, 14124 (2015).
9. S. Mishra, S. Srinivasan, C. Ma, N. Zhang, CD8+ Regulatory T Cell – A Mystery to Be Revealed. *Front. Immunol.* **12**, 3374 (2021).
10. Y. Kiniwa, Y. Miyahara, H. Y. Wang, W. Peng, G. Peng, T. M. Wheeler, T. C. Thompson, L. J. Old, R.-F. Wang, CD8+ Foxp3+ Regulatory T Cells Mediate Immunosuppression in Prostate Cancer. *Clin. Cancer Res.* **13**, 6947–6958 (2007).
11. N. Chaput, S. Louafi, A. Bardier, F. Charlotte, J.-C. Vaillant, F. Ménégaux, M. Rosenzwajg, F. Lemoine, D. Klatzmann, J. Taieb, Identification of CD8+CD25+Foxp3+ suppressive T cells in colorectal cancer tissue. *Gut* **58**, 520–529 (2009).
12. G. Churlaud, F. Pitoiset, F. Jebbawi, R. Lorenzon, B. Bellier, M. Rosenzwajg, D. Klatzmann, Human and Mouse CD8+CD25+FOXP3+ Regulatory T Cells at Steady State and during Interleukin-2 Therapy. *Front. Immunol.* **6** (2015).
13. C. E. Whyte, K. Singh, O. T. Burton, M. Aloulou, L. Kouser, R. V. Veiga, A. Dashwood, H. Okkenhaug, S. Benadda, A. Moudra, O. Bricard, S. Lienart, P. Bielefeld, C. P. Roca, F. J. Naranjo-Galindo, F. Lombard-Vadnais, S. Junius, D. Bending, T. Hochepied, T. Y. F. Halim, S. Schlenner, S. Lesage, J. Dooley, A. Liston, Context-dependent effects of IL-2 rewire immunity into distinct cellular circuits. *J. Exp. Med.* **219**, e20212391 (2022).
14. L. B. Jarvis, M. K. Matyszak, R. C. Duggleby, J. C. Goodall, F. C. Hall, J. S. H. Gaston, Autoreactive human peripheral blood CD8+ T cells with a regulatory phenotype and function. *Eur. J. Immunol.* **35**, 2896–2908 (2005).
15. A. Liston, M. Aloulou, A fresh look at a neglected regulatory lineage: CD8+Foxp3+ Regulatory T cells. *Immunol. Lett.* **247**, 22–26 (2022).
16. D. Simone, F. Penkava, A. Ridley, S. Sansom, M. H. Al-Mossawi, P. Bowness, Single cell analysis of spondyloarthritis regulatory T cells identifies distinct synovial gene expression patterns and clonal fates. *Commun. Biol.* **4**, 1395 (2021).
17. M. S. Vacchio, R. Bosselut, What Happens in the Thymus Does Not Stay in the Thymus: How T Cells Recycle the $CD4^+$–$CD8^+$ Lineage Commitment Transcriptional Circuitry To Control Their Function. *J.*

Immunol. **196**, 4848–4856 (2016).
18. Y. Fujii, M. Okumura, K. Inada, K. Nakahara, H. Matsuda, CD45 isoform expression during T cell development in the thymus. *Eur. J. Immunol.* **22**, 1843–1850 (1992).
19. P. A. Szabo, M. Miron, D. L. Farber, Location, location, location: Tissue resident memory T cells in mice and humans. *Sci. Immunol.* **4** (2019).
20. B. V. Kumar, W. Ma, M. Miron, T. Granot, R. S. Guyer, D. J. Carpenter, T. Senda, X. Sun, S.-H. Ho, H. Lerner, A. L. Friedman, Y. Shen, D. L. Farber, Human Tissue-Resident Memory T Cells Are Defined by Core Transcriptional and Functional Signatures in Lymphoid and Mucosal Sites. *Cell Rep.* **20**, 2921–2934 (2017).
21. S. Koizumi, H. Ishikawa, Transcriptional Regulation of Differentiation and Functions of Effector T Regulatory Cells. *Cells* **8**, 939 (2019).
22. S. N. Mueller, L. K. Mackay, Tissue-resident memory T cells: local specialists in immune defence. *Nat. Rev. Immunol.* **16**, 79–89 (2016).
23. N. Sugimoto, Y.-J. Liu, DUSP4 Stabilizes FOXP3 Expression In Human Regulatory T Cells. *Blood* **122**, 3473 (2013).
24. M. Delacher, C. D. Imbusch, A. Hotz-Wagenblatt, J.-P. Mallm, K. Bauer, M. Simon, D. Riegel, A. F. Rendeiro, S. Bittner, L. Sanderink, A. Pant, L. Schmidleithner, K. L. Braband, B. Echtenachter, A. Fischer, V. Giunchiglia, P. Hoffmann, M. Edinger, C. Bock, M. Rehli, B. Brors, C. Schmidl, M. Feuerer, Precursors for Nonlymphoid-Tissue Treg Cells Reside in Secondary Lymphoid Organs and Are Programmed by the Transcription Factor BATF. *Immunity* **52**, 295-312.e11 (2020).
25. M. Delacher, M. Simon, L. Sanderink, A. Hotz-Wagenblatt, M. Wuttke, K. Schambeck, L. Schmidleithner, S. Bittner, A. Pant, U. Ritter, T. Hehlgans, D. Riegel, V. Schneider, F. K. Groeber-Becker, A. Eigenberger, C. Gebhard, N. Strieder, A. Fischer, M. Rehli, P. Hoffmann, M. Edinger, T. Strowig, J. Huehn, C. Schmidl, J. M. Werner, L. Prantl, B. Brors, C. D. Imbusch, M. Feuerer, Single-cell chromatin accessibility landscape identifies tissue repair program in human regulatory T cells. *Immunity*, doi: 10.1016/j.immuni.2021.03.007 (2021).
26. R. Zhang, K. Xu, Y. Shao, Y. Sun, J. Saredy, E. Cutler, T. Yao, M. Liu, L. Liu, C. Drummer IV, Y. Lu, F. Saaoud, D. Ni, J. Wang, Y. Li, R. Li, X. Jiang, H. Wang, X. Yang, Tissue Treg Secretomes and Transcription Factors Shared With Stem Cells Contribute to a Treg Niche to Maintain Treg-Ness With 80% Innate Immune Pathways, and Functions of Immunosuppression and Tissue Repair. *Front. Immunol.* **11** (2021).
27. C. Domínguez Conde, C. Xu, L. B. Jarvis, D. B. Rainbow, S. B. Wells, T. Gomes, S. K. Howlett, O. Suchanek, K. Polanski, H. W. King, L. Mamanova, N. Huang, P. A. Szabo, L. Richardson, L. Bolt, E. S. Fasouli, K. T. Mahbubani, M. Prete, L. Tuck, N. Richoz, Z. K. Tuong, L. Campos, H. S. Mousa, E. J. Needham, S. Pritchard, T. Li, R. Elmentaite, J. Park, E. Rahmani, D. Chen, D. K. Menon, O. A. Bayraktar, L. K. James, K. B. Meyer, N. Yosef, M. R. Clatworthy, P. A. Sims, D. L. Farber, K. Saeb-Parsy, J. L. Jones, S. A. Teichmann, Cross-tissue immune cell analysis reveals tissue-specific features in humans. *Science* **376**, eabl5197 (2022).
28. THE TABULA SAPIENS CONSORTIUM, The Tabula Sapiens: A multiple-organ, single-cell transcriptomic atlas of humans. *Science* **376**, eabl4896 (2022).
29. V. Coppard, G. Szep, Z. Georgieva, S. K. Howlett, L. B. Jarvis, D. B. Rainbow, O. Suchanek, E. J. Needham, H. S. Mousa, D. K. Menon, F. Feyertag, K. T. Mahbubani, K. Saeb-Parsy, J. L. Jones, FlowAtlas.jl: an interactive tool bridging FlowJo with computational tools in Julia. bioRxiv [Preprint] (2023). https://doi.org/10.1101/2023.12.21.572741.
30. R. C. Ferreira, H. Z. Simons, W. S. Thompson, D. B. Rainbow, X. Yang, A. J. Cutler, J. Oliveira, X. Castro Dopico, D. J. Smyth, N. Savinykh, M. Mashar, T. J. Vyse, D. B. Dunger, H. Baxendale, A. Chandra, C. Wallace, J. A. Todd, L. S. Wicker, M. L. Pekalski, Cells with Treg-specific FOXP3 demethylation but low CD25 are prevalent in autoimmunity. *J. Autoimmun.* **84**, 75–86 (2017).
31. F. Sallusto, D. Lenig, R. Förster, M. Lipp, A. Lanzavecchia, Two subsets of memory T lymphocytes with distinct homing potentials and effector functions. *Nature* **401**, 708–712 (1999).
32. D. L. Woodland, J. E. Kohlmeier, Migration, maintenance and recall of memory T cells in peripheral tissues. *Nat. Rev. Immunol.* **9**, 153–161 (2009).
33. Y. C. Kim, R. Bhairavabhotla, J. Yoon, A. Golding, A. M. Thornton, D. Q. Tran, E. M. Shevach, Oligodeoxynucleotides stabilize Helios-expressing Foxp3+ human T regulatory cells during in vitro expansion. *Blood* **119**, 2810–2818 (2012).

34. J. Jacobse, J. Li, E. H. H. M. Rings, J. N. Samsom, J. A. Goettel, Intestinal Regulatory T Cells as Specialized Tissue-Restricted Immune Cells in Intestinal Immune Homeostasis and Disease. *Front. Immunol.* **12** (2021).
35. L. B. Jarvis, D. B. Rainbow, V. Coppard, S. K. Howlett, Z. Georgieva, J. L. Davies, H. K. Mullay, J. Hester, T. Ashmore, A. Van Den Bosch, J. T. Grist, A. J. Coles, H. S. Mousa, S. Pluchino, K. T. Mahbubani, J. L. Griffin, K. Saeb-Parsy, F. Issa, L. Peruzzotti-Jametti, L. S. Wicker, J. L. Jones, Therapeutically expanded human regulatory T-cells are super-suppressive due to HIF1A induced expression of CD73. *Commun. Biol.* **4**, 1186 (2021).
36. H. Nunes-Cabaço, Í. Caramalho, N. Sepúlveda, A. E. Sousa, Differentiation of human thymic regulatory T cells at the double positive stage. *Eur. J. Immunol.* **41**, 3604–3614 (2011).
37. A. M. Thornton, P. E. Korty, D. Q. Tran, E. A. Wohlfert, P. E. Murray, Y. Belkaid, E. M. Shevach, Expression of Helios, an Ikaros transcription factor family member, differentiates thymic-derived from peripherally induced Foxp3+ T regulatory cells. *J. Immunol. Baltim. Md 1950* **184**, 3433–3441 (2010).
38. A. M. Thornton, J. Lu, P. E. Korty, Y. C. Kim, C. Martens, P. D. Sun, E. M. Shevach, Helios+ and Helios- Treg subpopulations are phenotypically and functionally distinct and express dissimilar TCR repertoires. *Eur. J. Immunol.* **49**, 398–412 (2019).
39. L. Morina, M. E. Jones, C. Oguz, M. J. Kaplan, A. Gangaplara, C. D. Fitzhugh, C. G. Kanakry, E. M. Shevach, M. Buszko, Co-expression of Foxp3 and Helios facilitates the identification of human T regulatory cells in health and disease. *Front. Immunol.* **14**, 1114780 (2023).
40. J. Choi, B.-R. Kim, B. Akuzum, L. Chang, J.-Y. Lee, H.-K. Kwon, TREGking From Gut to Brain: The Control of Regulatory T Cells Along the Gut-Brain Axis. *Front. Immunol.* **13** (2022).
41. J. B. Wing, Y. Kitagawa, M. Locci, H. Hume, C. Tay, T. Morita, Y. Kidani, K. Matsuda, T. Inoue, T. Kurosaki, S. Crotty, C. Coban, N. Ohkura, S. Sakaguchi, A distinct subpopulation of CD25− T-follicular regulatory cells localizes in the germinal centers. *Proc. Natl. Acad. Sci. U. S. A.* **114**, E6400–E6409 (2017).
42. A. M. Krieg, TLR9 and DNA “feel” RAGE. *Nat. Immunol.* **8**, 475–477 (2007).
43. J. Tian, A. M. Avalos, S.-Y. Mao, B. Chen, K. Senthil, H. Wu, P. Parroche, S. Drabic, D. Golenbock, C. Sirois, J. Hua, L. L. An, L. Audoly, G. La Rosa, A. Bierhaus, P. Naworth, A. Marshak-Rothstein, M. K. Crow, K. A. Fitzgerald, E. Latz, P. A. Kiener, A. J. Coyle, Toll-like receptor 9–dependent activation by DNA-containing immune complexes is mediated by HMGB1 and RAGE. *Nat. Immunol.* **8**, 487–496 (2007).
44. S. Ivanov, A.-M. Dragoi, X. Wang, C. Dallacosta, J. Louten, G. Musco, G. Sitia, G. S. Yap, Y. Wan, C. A. Biron, M. E. Bianchi, H. Wang, W.-M. Chu, A novel role for HMGB1 in TLR9-mediated inflammatory responses to CpG-DNA. *Blood* **110**, 1970–1981 (2007).
45. J. A. Hall, N. Bouladoux, C. M. Sun, E. A. Wohlfert, R. B. Blank, Q. Zhu, M. E. Grigg, J. A. Berzofsky, Y. Belkaid, Commensal DNA Limits Regulatory T Cell Conversion and Is a Natural Adjuvant of Intestinal Immune Responses. *Immunity* **29**, 637–649 (2008).
46. K. H. G. Mills, TLR9 Turns the Tide on Treg Cells. *Immunity* **29**, 518–520 (2008).
47. Z. Urry, E. Xystrakis, D. F. Richards, J. McDonald, Z. Sattar, D. J. Cousins, C. J. Corrigan, E. Hickman, Z. Brown, C. M. Hawrylowicz, Ligation of TLR9 induced on human IL-10–secreting Tregs by 1α,25-dihydroxyvitamin D3 abrogates regulatory function. *J. Clin. Invest.* **119**, 387–398 (2009).
48. H. Schmitt, J. Ulmschneider, U. Billmeier, M. Vieth, P. Scarozza, S. Sonnewald, S. Reid, I. Atreya, T. Rath, S. Zundler, M. Langheinrich, J. Schüttler, A. Hartmann, T. Winkler, C. Admyre, T. Knittel, C. Dieterich Johansson, A. Zargari, M. F. Neurath, R. Atreya, The TLR9 Agonist Cobitolimod Induces IL10-Producing Wound Healing Macrophages and Regulatory T Cells in Ulcerative Colitis. *J. Crohns Colitis* **14**, 508–524 (2020).
49. R. Atreya, L. Peyrin-Biroulet, A. Klymenko, M. Augustyn, I. Bakulin, D. Slankamenac, P. Miheller, A. Gasbarrini, X. Hébuterne, K. Arnesson, T. Knittel, J. Kowalski, M. F. Neurath, W. J. Sandborn, W. Reinisch, CONDUCT study group, Cobitolimod for moderate-to-severe, left-sided ulcerative colitis (CONDUCT): a phase 2b randomised, double-blind, placebo-controlled, dose-ranging induction trial. *Lancet Gastroenterol. Hepatol.* **5**, 1063–1075 (2020).
50. F. Noyan, K. Zimmermann, M. Hardtke-Wolenski, A. Knoefel, E. Schulde, R. Geffers, M. Hust, J. Huehn, M. Galla, M. Morgan, A. Jokuszies, M. P. Manns, E. Jaeckel, Prevention of Allograft Rejection by Use of Regulatory T Cells With an MHC-Specific Chimeric Antigen Receptor. *Am. J. Transplant. Off. J. Am. Soc. Transplant. Am. Soc. Transpl. Surg.* **17**, 917–930 (2017).

51. S. Bézie, B. Charreau, N. Vimond, J. Lasselin, N. Gérard, V. Nerrière-Daguin, F. Bellier-Waast, F. Duteille, I. Anegon, C. Guillonneau, Human CD8+ Tregs expressing a MHC-specific CAR display enhanced suppression of human skin rejection and GVHD in NSG mice. *Blood Adv.* **3**, 3522–3538 (2019).
52. D. Rainbow, S. Howlett, L. Jarvis, J. Jones, Multi tissue processing for single cell sequencing of human immune cells. (2021).
53. E. A. Moskalev, M. G. Zavgorodnij, S. P. Majorova, I. A. Vorobjev, P. Jandaghi, I. V. Bure, J. D. Hoheisel, Correction of PCR-bias in quantitative DNA methylation studies by means of cubic polynomial regression. *Nucleic Acids Res.* **39**, e77 (2011).
54. P. M. Warnecke, C. Stirzaker, J. R. Melki, D. S. Millar, C. L. Paul, S. J. Clark, Detection and measurement of PCR bias in quantitative methylation analysis of bisulphite-treated DNA. *Nucleic Acids Res.* **25**, 4422–4426 (1997).
55. J. T. Grist, L. B. Jarvis, Z. Georgieva, S. Thompson, H. K. Sandhu, K. Burling, A. Clarke, S. Jackson, M. Wills, F. A. Gallagher, J. L. Jones, Extracellular Lactate: A Novel Measure of T Cell Proliferation. *J. Immunol.*, doi: 10.4049/jimmunol.1700886 (2017).
56. K. Blighe, kevinblighe/EnhancedVolcano, (2020); https://github.com/kevinblighe/EnhancedVolcano.
57. Renesh Bedre, reneshbedre/bioinfokit: Bioinformatics data analysis and visualization toolkit, Zenodo (2020); https://doi.org/10.5281/zenodo.3841708.

Acknowledgements

We thank the deceased organ donors, donor families, and the extended Cambridge Biorepository for Translational Medicine (CBTM) team for access to the tissue samples. We also thank David Menon, Edward Needham, Menna Clatworthy and Alasdair Coles for access to additional blood and tissue samples. We acknowledge and were grateful for the support received from the Cambridge NIHR BRC cell phenotyping hub (Dept. Medicine, University of Cambridge) for this project.

Funding

This work was part funded by the Wellcome Trust (grants 105924/Z/14/Z;RG79413, RG93172/JONES/42203 and 220554/Z/20/Z), Chan Zuckerberg Initiative seed network (CZIF2019-002452 to JLJ) and the NIHR Cambridge Biomedical Research Centre (BRC-1215-20014). For the purpose of open access, the authors have applied a CC BY public copyright licence to any Author Accepted Manuscript version arising from this submission. The views expressed here are those of the author(s) and not necessarily those of the NIHR, or Department of Health and Social Care.

Supplementary Materials:

Materials and Methods
Supp Figs. S1 to S24
Table S1

Materials and Methods

Ethics Statement:

All work was completed under ethically approved studies. Human PBMCs were isolated from healthy volunteers after obtaining fully informed consent under CAMSAFE (REC-11/33/0007) or CAMREG (21/NS/0011) and from leukocyte cones or cord blood of healthy donors (NHSBT, UK) or from in-patients under REC 97/290. Human tissues were obtained from deceased transplant organ donors via the Cambridge Biorepository for Translational Medicine (CBTM) (REC 15/EE/0152 REC: East of England-Central Cambridge Research Committee). Additional kidneys were provided under REC12/EE/0446.

Cell isolation and Magnetic separation:

Human PBMCs were isolated from heparinised blood and tissue derived mononuclear cells were isolated from mechanically dissociated and filtered human tissue using Ficoll density gradient centrifugation (Ficoll PaquePlus; GE Healthcare, Amersham) or 33% Percoll (GE Healthcare) as previously described(*27*). Solid tissues were mechanically dissociated following enzymatic treatment with either Liberase TL (Roche) or collagenase IV (Sigma) where appropriate. For a detailed protocol please refer to protocols.io(*52*). Prior to flow sorting Tregs, untouched Pan T cells were enriched by negative selection using T cell isolation kit II (Miltenyi biotec). All donor tissue information is included in Table S1.

Flow phenotyping and flow sorting:

Cells were stained using a range of antibodies (BD, eBioscience, Biolegend) at 1:50 dilution unless otherwise stated, and blocked using 3% FCS or mouse serum in Facs buffer and/or Tru block monocyte blocker (Biolegend) as required. Intracellular staining was performed using the FOXP3 permeabilization staining kit (Invitrogen) for 45 minutes at room temperature followed by staining of intracellular markers in 1x perm wash buffer for 45 minutes at room temperature. Dual-fluorochrome CD25 staining was performed by staining surface CD25 using two CD25 antibodies (clones MA2.1/2A3) on BB515 at saturating concentration, washing cells x 3 with Facs buffer to remove excess surface antibody and then staining intracellular CD25 post perm/fix using antibodies of the same two clones on a second fluorochrome (APC). Cell sorting was performed on either a FACS Aria (BD) or Influx (BD) cell sorter. Flow acquisition for phenotyping was performed on the Canto II or Fortessa LSR (BD Biosciences) and analysed using FlowJo v7.6.5-v10.0 (Tree Star Inc) or FlowAtlas(*29*). All antibodies and flow panels are detailed in Table S1.

Ex vivo Treg isolation and expansion:

Human *ex vivo* CD3+CD127^{lo}CD25^{+}CD4^{+} , CD3+CD127^{lo}CD25^{+}CD8+ or bulk CD3+ CD127^{lo}CD25^{+} were flow sorted from human blood, spleen, LN or gut MNCs (after a period of resting at 37oC in X-vivo 15 continuing 1% human AB serum) using a BD FACSAria cell sorter (BD Biosciences, see supplementary table 1 for sort

and flow panels). Cells were collected for TSDR demethylation analysis and stored at -80 as cell pellets or expanded with 500-1000 U/mL human rIL2 (Miltenyi Biotec/Chiron) +/- 100 nM rapamycin (Miltenyi Biotec) and human Treg expansion kit anti-CD3/CD28 beads (Miltenyi Biotec/Invitrogen), using x-vivo 15 cell medium (Lonza) tissue culture medium supplemented with L-glutamine, penicillin-streptomycin (both PAA Laboratories, UK), HEPES (Gibco, UK) and 1-3% human AB pooled serum and media exchanged with fresh IL-2 every 3-5 days. For additional expansion periods Grex cell culture flasks were used (Wilson Wolf). Beads were removed using MACSibead magnet (Milteny Biotec) prior to phenotyping or use in functional assays.

Measurement of *FOXP3* TSDR methylation:

The methylation status of the *FOXP3* TSDR was measured using the protocol previously(*35*). In brief, Tregs or control Teffector cells, were processed with the Qiagen Epitect Fast Bisulfite kit, which lyses the cells and performs the bisulfite conversion in a single step. First round PCR targeted 9 CpG sites within the *FOXP3* TSDR and a second round PCR added index sequences and illumina compatible ends allowing for sequencing on an Illumina MiSeq (2x300 bp reads). The percent FOXP3 TSDR demethylation was calculated as the proportion of sequencing reads containing 8 or 9 of the CpG sites within the TSDR being demethylated compared to the total number of sequencing reads. For female donors TSDR demethylation values were multiplied by two to account for the fact that one X chromosome is fully methylated due to X inactivation as FOXP3 is located on the X chromosome. Since there is a known bias in PCR efficiency of demethylated DNA(*53*, *54*) this leads to values of over 100% TSDR demethylation being measured in female donors. For Treg samples with less than 10,000 cells, flow sorted FOXP3- B cells were added to bring the total cell count to 10,000 (i.e. within the optimal cell number range for the methylation assay). The dilution factor was used to adjust the TSDR methylation value obtained.

***In vitro* stimulation and suppression assays:**

For short term activation of sorted Tregs and Teffs, cells were cultured in RPMI complete media containing 10% FCS, Penicillin-streptomycin and Hepes +/- anti-CD3/CD28 stimulation (Invitrogen Dynabeads) at a cell:bead ratio of 4:1. *In vitro* suppression assays were performed as previously described(*35*, *55*), briefly: efluor670 (Invitrogen) labelled Tregs (*ex vivo* or expanded) and cell tracker efluor450 (Invitrogen) labelled MACS sorted Pan T cells (Miltenyi T cell isolation kit II) were co-cultured in 96V bottom plates (Greiner). Pan Teffs were seeded at $2x10^4$ cells per well in RPMI+ 3% human AB serum in the absence or presence of equal and titrated numbers of Tregs and stimulated using Miltenyi Tregs suppression inspector beads according to the manufacturer's instructions. Stocks of allogeneic pan Teffs pre-labelled with efluor450 cell tracker dye were frozen in liquid nitrogen and used as standard Teffs for these assays. Proliferation was measured on day 4-5 using BD Fortessa HTS plate reader. $V670^+$ Tregs were gated out to enable analysis of the effector population ($CD4^+efluor450^+efluor670^-$ cells) and suppression was calculated by taking the ratio between the proliferating and non-proliferating populations as previously described(*35*, *55*)

Transcriptomic profiling by Nanostring

15,000 freshly-sorted *ex vivo* CD8 Tregs, CD4 Tregs and DP Tregs and equivalent effector cell populations +/- were harvested and washed twice in PBS, cells pelleted and lysed in RLT buffer (Qiagen). RNA was extracted using Qiagen RNeasy micro kit and their transcriptome measured using the nanostring Human Immunology V2 characterisation panel (Nanostring technologies) using an nCounter prep station and digital analyser.

Cytokine Analysis

Cytokines were measured in cell culture supernatants using luminex analysis (Biorad human 17-plex Bioplex kit) according to the manufacturer's instructions. Briefly, cell culture supernatants were harvested either from expanding CD4 and CD8 Tregs or from suppression assay supernatants at day 5, and stored in -80 until used. Upon thawing, supernatants were used either neat or diluted 1:2, and plated in duplicates. 17 human cytokines were analysed simultaneously using the kit and run on the Luminex analyser (BIORAD), standard curves for each cytokine created and per cytokine concentrations calculated using the BioRad software.

Statistics and Reproducibility:

All flow cytometry data were analysed using FlowJo (version 10). Statistical tests were performed using GraphPad Prism 6.0 software (GraphPad Software Inc, California). Comparisons between groups of three or more were compared using a one way ANOVA with Tukey's or Dunnet's post-hoc multiple comparisons tests, as indicated. Comparisons of 2 groups were tested with either one-tailed or two-tailed Student's t-tests, a two-way ANOVA with Bonferroni post-hoc multiple comparisons test, or multiple T-tests with Holm-Sidak post-hoc correction as appropriate. The number of biological replicates for each data set are given in figure legends.

Nanostring data were normalised using nSolver 4.0 software (Nanostring), background thresholding was performed at the mean+2SD of the negative probe values for each sample (range 15.2 - 36.4). Only probes with counts greater than the background threshold in at least 2 of the 3 samples were included in the analysis. Volcano plots were generated using the EnhancedVolcano R package(*56*) and heatmaps were visualised with the Bioinfokit Python package(*57*).

Data Availability

All flow cytometry panels, donor information/metadata and raw data used to generate figures are available in Table S1. All other raw data are available from the corresponding author upon reasonable request.